Heliyon 6 (2020) e05219

Contents lists available at ScienceDirect

Heliyon

journal homepage: www.cell.com/heliyon

Research article

Statistical optimization of textile dye effluent adsorption by *Gracilaria edulis* using Plackett-Burman design and response surface methodology

R. Venkataraghavan, R. Thiruchelvi *, D. Sharmila

Department of Bio-Engineering, School of Engineering, Vels Institute of Science, Technology and Advanced Studies, Chennai 600117, India

ARTICLE INFO

Keywords:
Gracilaria edulis
Plackett-Burman design
Box-Behnken design
Decolorization
Desorption
Engineering
Materials science
Chemistry
Environmental science

ABSTRACT

Statistical optimization models were employed to optimize the adsorption of textile dye effluent onto *Gracilaria edulis*. Significant factors responsible for adsorption were determined using Plackett-Burman design (PBD) and were time, pH, and dye concentration. Box-Behnken (BB) design was used for further optimization. The predicted and the experimental values were found to be in good agreement, the coefficient of determination value 0.9935 and adjusted coefficient of determination value 0.9818 indicated that the model was significant. The results of predicted response optimization showed that maximum decolorization could be attained with time 131.51 min, pH 7.48, and dye concentration 23.13%. The model was validated experimentally with 92.65% decolorization efficiency. The experiment was confirmed using Fourier transform infrared spectroscopy (FTIR), high-resolution scanning electron microscope coupled with energy dispersive X-ray analysis (HR-SEM-EDX), X-ray diffraction spectrometry (XRD) and Brunauer-Emmett-Teller (BET) surface area and pore size analysis techniques. Desorption studies at various pH (2–14) were performed and a maximum of 23% of the dye was recovered from the adsorbed biomass.

1. Introduction

Environmental pollution is an alarming problem in developing countries. The textile industry is one of the largest and rapidly developing industries in the world. A dye is a colored substance used in many industries such as the textile industry, leather, cosmetics, paints, food, ceramics, construction wax, paper, etc. The environmental problem such as water and soil pollution are mainly due to the release of untreated textile dyes from the industries, surface runoffs, and sewage leakage and overflows (Piai et al., 2020). The release of textile effluent from the textile industry contains a complex mixture chemical, dyes, starch, detergents, heavy metals, biological oxygen demand (BOD), chemical oxygen demand (COD), and sulphates. The effluent from industries are generally strong-smelling, hot, and colored due to the presence of toxic chemicals (Ghaly et al., 2014; Harrelkas et al., 2009). The dyes and the chemicals are released into water bodies which change the nature of the water making them unfit for human use and agricultural purposes. It also affects the plants and animals present in the water bodies by inhibiting the penetration of sunlight into the water stream. The main concern of the textile industry is the release of highly toxic chemicals and the quantity of effluent into the environment causing serious damage to human life and the ecosystem. The treatment of textile dye is difficult due to the presence of detergents and other additives which make them into a complex structure and the effluent is resistant to light, oxygen, acids, and bases. The treatment of wastewater containing dyes is difficult since they have complex aromatic molecular structures which make them more stable. The treatment of the effluent can be done by physical, chemical, and biological methods (Kabbout and Taha, 2014) such as electrochemical treatment like electro-reduction, electrolysis, chemical precipitation, aeration, coagulation, advanced oxidation process using hydrogen peroxide or ozone and UV light to produce OH^- free radicals scavengers, membrane filtration, nano-filtration using nano-sized membranes, aerobic biological treatment using anaerobic microorganisms and non-aerobic biological treatment (Dasgupta J et al., 2015). These methods are complex in design, automatic, rapid, and high rates of accuracy compared to decolorization using adsorption. The predominant drawback is that these techniques are non-cost-effective, fouling of membrane, high electricity cost, sludge formation, and health hazards are a matter of concern (Parmar and Shukla, 2018). The biological method is eco-friendlier, non-labor-intensive, and requires low-cost investment and is easy to perform. This is accomplished by the use of dead biomass of plants, bacteria, fungi, algae, and yeast (Vijayaraghavan et al.,

* Corresponding author.
E-mail address: thiruchelvi.se@velsuniv.ac.in (R. Thiruchelvi).

https://doi.org/10.1016/j.heliyon.2020.e05219
Received 11 January 2019; Received in revised form 28 June 2020; Accepted 8 October 2020

2013). Biological treatment requires a large surface area, proper maintenance, and operation.

Adsorption technique is a simple and effective way for the removal of dye from wastewater. Biosorbent is employed to decolorize the bleaching colored water (Kabbout and Taha, 2014). Various natural adsorbents are cost-effective such as agricultural waste, cotton waste, rice husk, dead algal, and fungal biomasses, activated charcoal, and clay that act as potential biosorbents (da Cunha Oliveira, 2016; Romauld et al., 2019). Apart from these adsorbents, agricultural wastes such as apricot stone, cauliflower leaves, fruit peels, coir pith, corn cobs, tree bark, straw, ash, *Eugenia umbelliflora*, and *Ficus carica* are potentially used as important low-cost, naturally occurring, and renewable adsorbents (Dubey and Shiwani, 2012; Kharat, 2015). Sawdust, rise husk, sugarcane bagasse, pistachio shell, *Araucaria angustifolia* bark, pine needles, and bamboo sawdust are examples of some agricultural waste biomass that have been reported against various synthetic dyes (Georgin et al., 2018; Giusto et al., 2017; Hammud et al., 2015; Zhang et al., 2015). Also, timber waste, fruit peels like orange, banana, lime, coir pith, coconut husk, tea cake waste, coffee waste, and seaweeds (Chen et al., 2011; Gupta and Nayak, 2012; Machado et al., 2011; Popoola, 2019). Agricultural wastes are rich in negatively charged functional groups like carboxyl and hydroxyl enabling them to adsorb cationic dyes and heavy metals from aqueous solutions. Studies reported that pre-treatment using formaldehyde and acids enhanced adsorption efficiency by increasing the surface pore size (Khan and Nazir, 2015). Chitosan is a polymer derived from marine sources like brine shrimps, crabs, and terrestrial insects. Chitosan is a low-cost, non-toxic biosorbent possessing high adsorption affinity towards cationic dyes due to the presence of hydroxyl, amino, and carboxyl functional groups. Adsorption in chitosan is achieved through protonation of the amino-functional group resulting in electrostatic interaction between dye and chitosan (Vakili et al., 2014). Chitosan nanocomposites are very versatile in the application in the field of biotechnology in targeted drug delivery and environmental applications like heavy metal adsorption due to electrostatic interactions (Sharma et al., 2017).

Chemically modified adsorbent like nitrogen-modified titanium dioxide reported by Janus et al. (2008) is one of the promising adsorbents for the removal of dyes from aqueous solutions. The main pitfall is that the adsorbent is not cost-effective. Hydrogel-based adsorbents such as cross-linked and uncross linked polyacrylic acid, super-adsorbent nanocomposite hydrogels that are of nanometer-scale are also potential adsorbents for removing dyes from aqueous solutions. They are rich in functional groups on their surface like alcohol, amides, and carboxylic acids and are non-toxic, hydrophilic making them more stable. Nanocomposites of hydrogel and hydrocolloids such as nano synthesized agar, alginate, carrageenan, chitin, gelatin, and starch are some of the polymers that have wide applications in environmental and medical applications (Sharma et al., 2018). However, they are not cost-effective and are tedious in preparation compared to algae-based adsorbents. Moreover, their efficiency is much lower compared to other natural adsorbents (Hu et al., 2018). Zeolites and clays are abundant microporous hydrous aluminosilicates mineral adsorbents used predominantly for the adsorption of heavy metals and dyes from aqueous solutions due to the cationic and anionic electrostatic interactions between them (Ngulube et al., 2017; Wang and Peng, 2010). The high dispersive nature of clay and zeolites makes reusability studies difficult (Xu et al., 2012). Smectite rich clays, mesoporous zeolites, graphene oxide composites, mesoporous kaolin-based silica, magnesium phyllosilicates, and cellulose hydrogel are some of the natural clay and zeolite-based composites commonly used as adsorbents (Briao et al., 2018; Chaari et al., 2019; Li et al., 2015; Moscofian et al., 2012; Yang et al., 2019). Gum arabic, a natural polymer composed of repetitive units of 1,3-linked β-D-galactopyranosyl has versatile applications in environmental applications because since they are cheaper, reusable, and highly efficient in remediation (Sharma et al., 2018). Nanocomposites of biopolymers using silver, strontium, cerium, bi, and trimetallic and graphene oxides have been widely used as adsorbents, photocatalysts, electrochemical catalysts and ion exchangers tailoring environmental applications with promising results (Iftekhar et al., 2018; Kang et al., 2016; Sharma et al., 2018, 2019). Organic and synthetic dyes, heavy metals, pesticides, and polyphenols have been remediated through polymers through the process of adsorption, photocatalysis, and biological remediation (Dhiman et al., 2017; Haroon et al., 2018; Piai et al., 2020; Sui et al., 2016). Nanocomposites of anionic surfactant sodium dodecyl sulphate-iron silico phosphate are efficient in adsorbing cationic heavy metals and dyes from aqueous solutions because of their selective ion exchange capability and stability (Sharma et al., 2017). Thus, adsorption is more efficient than other remediation methods.

Calcium oxide and calcium sulphate are some of the low-cost effective chemical adsorbents used for the decolorization of dye effluent and heavy metals from aqueous solutions. However, the reusability is lower when compared to other natural adsorbents (Ramesh et al., 2017). Adsorbents are immobilized using sodium alginate and calcium chloride and used for the adsorption process promoting their reusability (Bai and Abraham, 2003).

Rhodophyta (red algae) is an economically important species and edible algae. Red algae occur in salt and freshwater environment and warmer conditions. *Gracilaria edulis* is a marine species that belongs to the class Florideophyceae and family Gracilarales. It contains a double cell wall and an outer layer that contains polysaccharide agarose and agaropectin (da Cunha Oliveira, 2016). It is a rich source of carrageenan, sulphates, glucose, and polyunsaturated fatty acids. Red algae have a high content of protein and low concentration of phenol group. The algal cell wall contains functional groups such as carboxyl, hydroxyl, and sulphate groups which act as a binding site for the charged dyes (Crist et al., 1981).

Biosorption of textile dye effluent is affected by diverse process parameters influencing the rate and efficiency of adsorption. It is mandatory to optimize the parameters for the effective degradation of dyes, especially at higher concentrations. These parameters include pH, temperature, dye concentration, biomass concentration, static-agitation, and time. The optimized parameters would definitely reduce the cost and the reaction time spent and increases the efficiency of biosorption (Priyadharshini and Bakthavatsalam, 2016). Hence, it is, therefore, necessary to optimize the parameters to maximize the adsorption of dye on to the alga species viz. *Gracilaria edulis*.

There are several methods for the optimization and modeling available from the ancient elementary model like one factorial at a time (OFAT) to composite and nexus statistical designs like Plackett-Burman design (PBD), Box-Behnken design (BB), and Central Composite Design (CCD) (Amara and Salem, 2010; Silveira et al., 2015). The OFAT was the most used in the ancient days to optimize the factors. This method was labor-intensive, time-consuming, and non-efficient due to interaction among the factors (Jo et al., 2008). Alternately, the statistical experiments could overcome the drawbacks associated with the (OFAT) and reduce the error in deducing the effect and interaction between factors (Suhaila et al., 2013). The Design of Experiments (DOE) propounds a minimum number of experimental trials. The DOE increases the efficiency of any process (Sivasubramanian and Namasivayam, 2015). PBD and Response surface methodology (RSM) (BB and CCD) designs are the most commonly used by the scientific communities for the process parameters optimization (Lakshmikandan et al., 2014; Agarry and Ogunleye, 2012).

Plackett Burman design is a very efficient method of screening to identify the significant factors among a large number of factors that influence a process using a few experimental runs (Ungureanu et al., 2015). RSM has been used importantly in various sectors and industries like product development, food industries, and bio-processing industries like bakeries and breweries through fermentation. RSM is an effective statistically designed methodology used to traverse the interactions between the independent variables and the dependent variables and predict the resultant responses in the presence of defined conditions (Jabeen

et al., 2015). The BB design permits the calculation of the responses at intermediate levels that were not been studied experimentally. The three-level BB design was commissioned in this study and the parameters were optimized with the minimum number of experimental trails compared to the other designs (Dong et al., 2009).

Therefore, the objective of the present research work was to obtain the significant parameters affecting the biosorption of textile dye effluent on to *Gracilaria edulis* using PBD and further optimizing the responses to maximize the efficiency of the process using the BB design and characterize them using sophisticated instrumentation techniques.

2. Materials and methods

All the chemicals used in this study were purchased from HiMedia laboratories and were of the highest purity. 0.1 N HCl and 0.1 M NaOH were prepared to adjust the pH of the solution.

2.1. Collection, authentication and preparation of biomass

The marine red macroalgae *Gracilaria edulis* was collected from the shallow intertidal zone along the Mandapam coast (Latitude: 9°16′32.56″ N & Longitude: 79°7′25.03″ E), Ramanathapuram district, Tamil Nadu. The confirmation and authentication of the species were done by Dr. M. Ganesan, Senior Scientist, Council of Scientific and Industrial Research - Central Salt and Marine Chemicals Research Institute (CSIR-CSMCRI), Mandapam Camp, Tamil Nadu. The algae were washed initially with water to remove the epiphytes and other contaminants and were packed in an air-tight polythene bag and was brought to the lab (Venkataraghavan and Thiruchelvi, 2019). Then the algae were washed with distilled water to remove the salts. The algae were shade dried for one week and crushed using mortar and pestle and further broken down with the help of an electric blender into small pieces. The biomass was sieved manually using a mesh sieve (size no: 18) to obtain a particle size of less than 1000 μm and stored in a clean dry place.

2.2. Collection and characterization of textile dye effluent

The textile dye effluent was obtained from a textile processing industry in Murugampalayam, Tiruppur, Tamil Nadu. The textile dye effluent was dark green in color with foul smell due to the mixture of several dyes like disperse dyes, direct dyes, cationic dyes, sulfur dyes, anionic dyes, and azoic dyes. The dyes were collected from the exit discharge of the industry. The effluent was stored in plastic bottles in a dark place under normal room temperature. The dye was analyzed between the ranges 800 to 200 nm spectrum in the (Shimadzu-1800) UV-Vis spectrophotometer and λ_{max} of the effluent was found to be 578.8 nm. The effluent was diluted to 10% (v/v) (10 mL of crude dye in 90 mL of distilled water), 20% (v/v) (20 mL of crude dye in 80 mL of distilled water), and 30% (v/v) (30 mL of crude dye in 70 mL of distilled water) using distilled water respectively and used for the experiment. The dye effluent was characterized for physicochemical analysis at Tamil Nadu testing labs, private limited, Chennai, and was reported in Table 1. The effluent was found to exceed the limits when compared to the Tamil Nadu pollution control board's standards for waste effluent discharge.

2.3. Pretreatment of biomass

Pretreatment of the biomass was done to enhance the biosorption of dye effluent on to the biomass. Physicochemical modifications of biomass could lead to the activation of binding sites resulting in better sorption uptake.

2.3.1. Physical pretreatment method

Physical treatment of the biomass was done using boiling water. 30 g of powdered biomass was added to add to 800 mL of 150 °C boiling water and was stirred continuously for 15 min. Then the biomass was filtered using Whatman filter paper (size 40) and a glass funnel to remove the water. The biomass was then dried in the hot air oven at 60 °C for 24 h (Zafar et al., 2013). Boiling water enhances the adsorption capacity of biomass by increasing the pore surface area.

2.3.2. Chemical method

2.3.2.1. Pretreatment using calcium chloride. 20 g of biomass was added to 500 mL of 0.2 M calcium chloride and the pH was adjusted to 5. The mixture was then shaken in an orbital shaker at 150 rpm for 24 h at 25 °C overnight for effective ion-exchange and complete crosslinking of alginic materials. The biomass was then washed with distilled water to remove traces of calcium chloride and dried in the hot air oven for drying at 60 °C for 24 h (Hanbali et al., 2014; Batzias and Sidiras, 2004).

2.3.2.2. Pretreatment using formaldehyde. 20 g of biomass was added to 170 mL 36% formaldehyde and 330 mL of 0.1 N hydrochloric acid. The mixture is shaken in orbital shaker for effective crosslinking and polymerization of alginic materials and was incubated in an orbital shaker at 150 rpm for 1 h. The biomass was then washed with distilled water to remove traces of formaldehyde and hydrochloric acid. The biomass then treated with 0.2 M Na_2CO_3 solution and again washed with distilled water. It was dried at 60 °C for 12 h and at 110 °C for 2 h (Leusch et al., 1995).

2.4. Experimentation

The optimization experiments were performed as batch adsorption studies in 250 mL Erlenmeyer flasks containing 100 mL of diluted dye effluent. The dye was diluted appropriately to respective concentrations using distilled water. The factor levels were maintained during the experiment. The adsorption studies were performed in the incubator for static conditions and the orbital shaker for agitated conditions. Constant agitation speed of 150 rpm was maintained throughout the study. On

Table 1. Characterization of textile dye effluent.

Parameter	Method	Unit	Result	TNPCB limits
pH at 25 °C	IS 3025 (Part 4)-1983 (RA.2017)/2120B APHA 23rd Edition 2017.	-	8.53	5.5–9.0
Chloride Cl^-	IS 3025 (Part 32)-1988 (RA.2014)/4500 Cl–B APHA 23rd Edition 2017.	mg/L	35361	Maximum 1000
Sulphate SO_4^{2-}	IS 3025 (Part 24)-1986 (RA.2014) 4500 SO_4^{2-} E APHA 23rd Edition 2017.	mg/L	54102	Maximum 1000
Total Dissolved Solids	IS 3025 (Part 16)-1984 (RA.2017)/2540C APHA 23rd Edition 2017.	mg/L	54102	Maximum 2100
Oil and Grease	IS 3025 (Part 39)-1991 (RA.2014)/5520 O&G B APHA 23rd Edition 2017.	mg/L	24	Maximum 10
COD (Open reflux method)	IS 3025 (Part 58)-2006 (RA.2017)/5220 B C APHA 23rd Edition 2017	mg/L	2870	Maximum 250
BOD at 27 °C for 3 days	IS 3025 (Part 44)-1993 (RA.2014).	mg/L	406	Maximum 30
Sodium as Na	IS 3025 (Part 45)-1993 (RA. 2014)/3500 Na–B APHA 23rd Edition 2017.	mg/L	11200	-
Potassium as K	-	-	1250	-
Sulphide S^-	APHA 4500 S2–F. 23rd Edition 2017.	mg/L	2.40	-

reaching equilibrium conditions, the effluent was centrifuged at 2500 rpm (Remi R–8C Laboratory Centrifuge) for 5 min to remove the biomass debris and the supernatant was preserved. The filtrate after each trial was analyzed using (Shimadzu UV-1800) UV-Vis spectrophotometer at 578.8 nm with sterile distilled water as blank and the readings were tabulated. Effluent without adding biomass was used as control. The decolorization percentage was calculated using the following equation (Eq. (1)).

$$Y = (Initial\ absorbance - Final\ absorbance\ /Initial\ absorbance) * 100 \quad (1)$$

where Y denotes the decolorization percentage.

2.5. Design of experiments

2.5.1. Screening of process parameters using Placket-Burman design (PBD)

The PBD is an effective method used for screening the significant factors from a large number of factors affecting the process (Zhou et al., 2011). The following first-order polynomial equation (Eq. (2)) was used to perform mathematical modeling.

$$Y = \beta_\circ + \Sigma\, \beta_\circ\, x_i \quad (2)$$

where Y denotes the predicted response (decolorization percentage), $\beta_\circ$ denotes the model intercept, β_i denotes the linear coefficient, and x_i denotes the level of each independent variable.

Six independent variables namely i) pH, ii) temperature, iii) dye concentration, iv) biomass concentration, v) static-agitation, and vi) time were investigated at 95% confidence level in a single replicate. The factors were varied according to the two-level PBD. PBD matrix was developed for 6 parameters with 12 experimental trials to shortlist the significant parameters that influence the biosorption by *Gracilaria edulis* (El-Naggar et al., 2018; Ungureanu et al., 2015). Every independent variable was assessed at lower (-) and higher (+) levels (Table 2).

Table 3 denotes the experimental design (factors and range) of the biosorption process using PBD. The factors having P-value lesser than 0.05 (confidence level greater than 95%) were considered to be significant and thus influence the decolorization process. The significant factors were further optimized using the Box-Behnken design of RSM.

2.5.2. Response surface methodology (RSM) using Box-Behnken design (BB) of experiments

Once after screening the significant factors using PBD, the RSM using the BB design was performed to obtain the details regarding the significant effects and to study the interactions between the shortlisted significant factors with a positive effect on the decolorization of the dye effluent and to determine the optimal value of every variable that would influence the decolorization of dye to the maximum.

Three factors were found to be significant from the PBD: i) time (minutes), ii) pH and iii) dye concentration (%) and were further optimized using BB design. Each significant factor or independent variable was evaluated at three disparate levels: center points (-, 0, +) (Table 4).

The decolorization of dye effluent was investigated using the second-order polynomial equation. The data were fitted on to the second-order equation by multiple regression method. The following second-order quadratic equation was used (Eq. (3)).

$$Y = \beta_0 + \beta_1 X_1 + \beta_2 X_2 + \beta_3 X_3 + \beta_{12} X_1 X_2 + \beta_{13} X_1 X_3 + \beta_{23} X_2 X_3 + \beta_{11} {X_1}^2 + \beta_{22} {X_2}^{2+}\, \beta_{33} {X_3}^2 \quad (3)$$

where Y denotes the predicted response (decolorization percentage); β_0 is the constant coefficient; β_1, β_2, β_3 denote the linear regression coefficients; β_{11}, β_{22}, β_{33} represent the quadratic regression coefficients; β_{12}, β_{13}, β_{23} represent the interaction coefficients and X_1, X_2, X_3 represent the coded values of significant independent variables.

The (Eq. (3)) gives the relationship of the response (Y) to significant variables X_1, X_2, and X_3. The quality of the second-order polynomial equation was evaluated statistically by Analysis of variance (ANOVA) which includes a coefficient of determination (R^2), and its statistical significance was scrutinized by Fischer's test (F-test). The coefficient of determination (R^2) was used to measure the goodness of fit of the model. The response contour and surface plots were studied. The contour and surface plots showed good interaction between the significant factors.

2.6. Analysis of data

Minitab18.1, Pennsylvania, U.S.A was used for the statistical and regression analysis of data. This software is chosen since it provides a very comprehensive and easy interpretation of results.

2.7. Characterization of biomass using fourier transform infrared spectroscopy, scanning electron microscopy coupled with energy dispersive X-ray analysis, X-ray diffraction spectrometry and Brunauer Emmett Teller surface area analysis

Fourier transform infrared spectroscopy (FTIR) was performed at Sophisticated Instrumentation Facility, Vellore Institute of Technology, Vellore. The spectra were analyzed by Thermo Electron Scientific using the KBr disc mode. The sample was mixed with 1% KBr and pressed into pellets and was analyzed in the mid-infrared region (400-4000 cm^{-1}) at 4 cm^{-1} resolution to obtain the spectra.

A high-resolution scanning electron microscope (HR-SEM) coupled with energy dispersive X-ray analysis (EDX) was used to analyze the morphology of biomass before and after adsorption. The analysis was performed at the Sophisticated Analytical Instruments Facility, Indian Institute of Technology, Madras using FEI Quanta 200 FEG-EDAX high-resolution scanning electron microscope. The samples were made electrically conducting by coating a layer of gold on their surface. The analysis after biosorption was carried out for the third trial of Box-Behnken design since it has the highest biosorption efficiency (Table 7).

X-ray diffraction spectrometry (XRD) was performed at Central Instrumentation Facility, Vels Institute of Science, Technology and Advanced Studies, Pallavaram. XRD was used to analyse the crystalline, amorphous nature, and mineral content of biomass (Zhou et al., 2018). The analysis was carried using Rigaku Smart Lab X-ray diffractometer using Cu-Kα radiation source, λ = 0.15406 Å at 45 kV and 40 mA in the 2θ range of 0–100°. The XRD data was compared with Mineralogy Database to identify the mineral composition (Table 9). The average crystallite size was calculated using the Debye-Scherrer equation (Holzwarth and Gibson, 2011).

Brunauer Emmett Teller (BET) and Barrett-Joyner-Halenda (BJH) for surface area and pore size analysis were performed at Central Instrumentation Facility, Vels Institute of Science, Technology and Advanced Studies, Pallavaram using BELSORP-max analyzer. The analysis was performed at low pressure ($1*10^{-8}$) using inert nitrogen at 77K and argon at 87K using a 13.3 Pa pressure transducer. The biosorbent was analyzed before and after adsorption to study the total surface area, total pore volume, and mean pore diameter. Adsorption-desorption isotherm and pore size distribution were

Table 2. Factor levels tested using Plackett-Burman Design.

Parameters	Experimental value	
	Low (-)	High (+)
pH	3	9
Temperature	20	40
Dye concentration	10	30
Biomass concentration	1	10
Static-Agitation	Static	Agitation
Time	120	180

Table 3. Experimental design of factors with experimental and predicted results using Plackett-Burman Design.

Run	pH	Temperature	Dye conc	Biomass conc	Static-Agitation	Time	Decolorization %	
							Experimental	Predicted
1	+	-	+	-	-	-	90.72	90.78
2	+	+	-	+	-	-	88.40	88.42
3	-	+	+	-	+	-	92.54	92.75
4	+	-	+	+	-	+	87.23	87.48
5	+	+	-	+	+	-	88.65	88.62
6	+	+	+	-	+	+	88.05	87.80
7	-	+	+	+	-	+	89.64	89.25
8	-	-	+	+	+	-	92.53	92.64
9	-	-	-	+	+	+	88.45	88.47
10	+	-	-	-	+	+	86.89	86.82
11	-	+	-	-	-	+	87.95	88.37
12	-	-	-	-	-	-	91.94	91.56

Table 4. Coded levels of factors evaluated using Box-Behnken (BB) design.

Factors	Coded levels		
	-	0	+
Time	120	150	180
pH	3	6	9
Dye concentration	10	20	30

plotted using inert gases under a vacuum environment, the saturated vapor pressure of 102.72 kPa conditions.

3. Results and discussion

3.1. Selection of significant factors influencing the decolorization of textile dye effluent using Plackett-Burman design (PBD)

PBD is an effective screening design used to identify the significant factors affecting the decolorization of textile dye effluents from a large number of candidate factors. It is a two-level fractional factorial design and is based on the first-order polynomial equation without any interaction among the independent factors (Plackett et al., 1946; Jabeen et al., 2015).

The influence of six important factors was statistically analyzed using the PBD. Three of the six factors namely i) time, ii) pH, and iii) dye concentration a have significant effect on the decolorization of the effluent. The factors with $P < 0.05$ (confidence levels>95%) were assumed to be significant and chosen for the next level of optimization by the Box-Behnken (BB) design of RSM. Multiple regression analysis was applied to the experimental results and fitted on to first-order polynomial equation represented as Y.

$$Y = 98.057 - 0.3642\ pH - 0.0211\ Temperature + 0.0702\ Dye\ conc - 0.0591\ Biomass\ conc + 0.103\ Static\text{-}agitation - 0.04603\ Time \quad (4)$$

where Y in Eq. (4) is the response (decolorization percentage). Table 5 denotes information about significant factors ($P < 0.05$). The value of the coefficient of determination (R^2) was found to be 0.9852 which indicated that 98.52% of variability could be explained by the selected model and could not explain only 1.48% of the total variability. Moreover, the predicted R^2 value of 0.9146 was found to be an inequitable agreement with the adjusted R^2 value of 0.9674 which denotes the validity of the model.

Table 6 shows the information about statistical analysis of experimental data using Fischer's test for Analysis of variance and provides detailed information about the T-values and P-values for each independent variable which served as tools to identify the significant factors affecting the process. The Model Fischer's value of 55.39 and the T-value of 845.25 were obtained.

A decrease in decolorization was observed when the time (coefficient value of -1.381) was increased from 120 to 180 min (- to +). Other factors such as pH, temperature, and biomass concentration (coefficient value of -1.093, -0.211, and -0.266) were also found to a exert negative effect on the decolorization process. Thus, by decreasing the time, pH, temperature, and biomass concentration were found to exert a positive effect on the dye decolorization process. On the other hand, the increase in dye concentration and static-agitation (coefficient value of 0.702 and 0.103) had positive effect on the decolorization process. Thus, by increasing the dye concentration could exert a positive effect on the dye decolorization. The maximum response of 92.54% (experimental) was obtained at pH 3; temperature 40 °C; dye concentration 30%; biomass concentration 1 g/L; agitated condition; and time 120 min in the third trial of PBD (Table 3).

Table 5. Statistical analysis of six factors using Plackett-Burman Design.

Term	Effect	Coef	SE Coef	T-Value	P-Value	VIF
Constant		89.416	0.106	845.25	0.000	
pH	-2.185	-1.093	0.106	-10.33	0.000	1.00
Temperature	-0.422	-0.211	0.106	-1.99	0.103	1.00
Dye conc	1.405	0.702	0.106	6.64	0.001	1.00
Biomass conc	-0.532	-0.266	0.106	-2.51	0.054	1.00
Static-Agitation	0.205	0.103	0.106	0.97	0.377	1.00
Time	-2.762	-1.381	0.106	-13.05	0.000	1.00

R2 = 0.9852; Adjusted R2 = 0.9674; Predicted R2 = 0.9146.

Table 6. Analysis of variance for experimental results using Plackett-Burman Design.

Source	DF	Adj SS	Adj MS	F-Value	P-Value
Model	6	44.6326	7.4388	55.39	0.000
Linear	6	44.6326	7.4388	55.39	0.000
pH	1	14.3227	14.3227	106.66	0.000
Temperature	1	0.5334	0.5334	3.97	0.103
Dye conc	1	5.9221	5.9221	44.10	0.001
Biomass conc	1	0.8480	0.8480	6.31	0.054
Static-Agitation	1	0.1261	0.1261	0.94	0.377
Time	1	22.8804	22.8804	170.38	0.000
Error	5	0.6714	0.1343		
Total	11	45.3041			

DF- Degrees of Freedom; Adj SS- Adjusted Sum of Squares; Adj MS- Adjusted Mean Square.

3.2. *Statistical process optimization of textile dye effluent decolorization by* Gracilaria edulis *using Box-Behnken (BB) design*

Significant factors obtained from the PBD namely i) time, ii) pH, and iii) dye concentration were further statistically optimized and studied using the three-level (-, 0, +) BB design. The experiment was performed in a single replicate. The levels of the factors were set based on the previous PBD. A matrix was designed with three variables containing coded and actual levels with their responses (decolorization percentage) were displayed in Table 7. Temperature, biomass concentration, and static-agitations exerted negative effect (insignificant factors) on the dye decolorization were set at their respective low levels of their PBD for further optimization. The BB design presented fifteen trials with experimental and predicted values for three factors (Table 7). Depending on the contrast in the three significant variables, the percentage of decolorization varied from 86.97% to 92.30% in the sixth and the third trials. The maximum decolorization potential was attained at the third trial with 92.30% decolorization at time 120 min; pH 9; dye concentration 20% (Table 7).

3.3. *Analysis of variance for box behnken design*

The analysis of variance of the model using second-order polynomial using BB design was tabulated (Table 8). According to Cui et al., a regression model with R^2 (coefficient of determination) value greater than 0.90 would possess a high correlation (Cui et al., 2010). The value of R^2 should not be lower than 0.74 until the model is appropriate (Le Man et al., 2010). Nevertheless, Koocheki et al. stated that higher values of R^2 do not mean that the regression model is moral and, in that case, the conclusion can be done depending upon a greater adjusted R^2 value Koocheki et al. (2009). The R^2 value for the model was found to be 0.9935 and the adjusted R^2 was 0.9818 which denoted a very good agreement between the experimental and the adjusted R^2 values. The coefficient of determination (R^2 = 0.9935) indicated that 99.35% of decolorization variability could be explained by the model. Moreover, the adjusted R^2 value (0.9818) was also found to be high denoting a greater significance of the model. The predicted R^2 value for the model was found to be 0.8958 which was also very high. Additionally, for a model to be significant, the predicted R^2 and the adjusted R^2 values must be less than 20% (Rai et al., 2016). In the present study, the predicted R^2 = 0.8958 was found to be in good agreement with the adjusted R^2 value of 0.9818 indicating the validity of the model and the model could explain 89.58% variability in predicting the decolorization of textile dye effluent in the range of experimental variables. The regression coefficients equation was calculated and the experimental data was suited on to the second-order polynomial equation (Eq. (5)). The equation obtained could describe the decolorization percentage.

$$Y = 65.29 + 0.1825\ Time + 2.384\ pH + 0.5454\ Dye\ conc - 0.000647\ Time*Time - 0.1322\ pH*pH - 0.02135\ Dye\ conc*Dye\ conc - 0.00758\ Time*pH + 0.001925\ Time*Dye\ conc + 0.02567\ pH*Dye\ conc \quad (5)$$

where Y represent the predicted decolorization percentage.

From Eq. (5), the highest regression coefficient was achieved by pH (2.384), followed by dye concentration (0.5454), followed by time

Table 7. Experimental design of factors with experimental and predicted results using Box-Behnken Design.

RunOrder	Time	pH	Dye conc	Decolorization %	
				Experimental	Predicted
1	-	-	0	89.65	89.62
2	+	-	0	89.60	89.87
3	-	+	0	92.30	92.02
4	+	+	0	89.52	89.54
5	-	0	-	88.95	89.11
6	+	0	-	86.97	86.84
7	-	0	+	90.52	90.64
8	+	0	+	90.85	90.68
9	0	-	-	87.77	87.62
10	0	+	-	87.02	87.12
11	0	-	+	88.87	88.76
12	0	+	+	91.20	91.34
13	0	0	0	92.04	92.04
14	0	0	0	92.04	92.04
15	0	0	0	92.04	92.04

Table 8. Analysis of variance using Box-Behnken (BB) design.

Source	DF	Adj SS	Adj MS	F-Value	P-Value
Model	9	45.8050	5.0894	84.77	0.000
Linear	3	19.0532	6.3511	105.79	0.000
Time	1	2.5088	2.5088	41.79	0.001
pH	1	2.1528	2.1528	35.86	0.002
Dye conc	1	14.3916	14.3916	239.72	0.000
Square	3	21.1829	7.0610	117.61	0.000
Time*Time	1	1.2528	1.2528	20.87	0.006
pH*pH	1	5.2287	5.2287	87.09	0.000
Dye conc*Dye conc	1	16.8304	16.8304	280.34	0.000
2-Way Interaction	3	5.5688	1.8563	30.92	0.001
Time*pH	1	1.8632	1.8632	31.04	0.003
Time*Dye conc	1	1.3340	1.3340	22.22	0.005
pH*Dye conc	1	2.3716	2.3716	39.50	0.001
Error	5	0.3002	0.0600		
Lack-of-Fit	3	0.3002	0.1001	*	*
Pure Error	2	0.0000	0.0000		
Total	14	46.1052			

DF- Degrees of Freedom; Adj SS- Adjusted Sum of Squares; Adj MS- Adjusted Mean Square.

(0.1825). All the factors had a net positive regression coefficient indicating a positive effect on the dye decolorization. Table 8 denotes the analysis of variance which is mandatory to analyze the adequacy and significance of the experimental model (Harrelkas et al., 2009). Analysis of variance splits the total variation into two distinct components namely i) variation affiliated with the model and ii) variation affiliated with the experimental error. The results from the analysis of variance show whether the model was significant or not when correlated with the variations affiliated with the residual (difference between the experimental and the predicted) error (Aleboyeh et al., 2008). The F-value gives the ratio between the mean square and the residual error of the model. From Table 8, the F-value was found to be 84.77 and the lack-of-fit value was found to be 0.1001. F-ratio of the model was found to be 84.77 which is greater than the tabulated F-value (F = 0.1001 at 95% significance) indicating the adequacy of the model. The T-value and the P-value were used as predominant tools used to evaluate the significance of every coefficient. Thus, the linear, quadratic, and interactive terms were found to be highly significant for the textile dye decolorization.

3.4. Surface and contour plots- interaction between the significant factors

The two-dimensional contour and three-dimensional surface plot were used to investigate the effect of the individual variables and their interaction for the predicted responses on the decolorization of dye effluent. Figures 1, 2, and 3 show the 2D contour and 3D surface plots. The plots were based on Eq. (5) where one variable was kept constant and the other two variables were altered inside the experimental range. The shape of the surface and its corresponding contour plot was important to study the mutual interactions between the variables. Each response surface plot (Figures 1, 2, and 3) denoted a clear peak in the center, which indicates that the optimum value point was within the experimental boundary level.

Figure 1 (a and b) shows the graphical representation indicating the combined effects of pH and time on dye decolorization while the dye concentration was set to its zero levels (Dye conc = 20%). From Figure 1 (a and b), it was clear that an increase in the pH could augment the decolorization of dye effluent (Y). The maximum decolorization was observed in the pH range 5.8–9. pH plays an important role in the

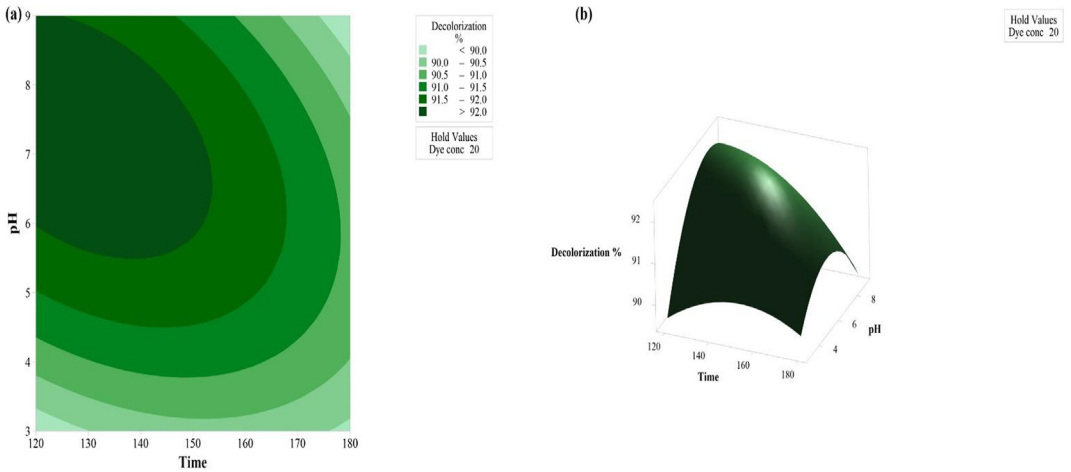

Figure 1. Contour plot and response surface plot showing interaction between time and pH.

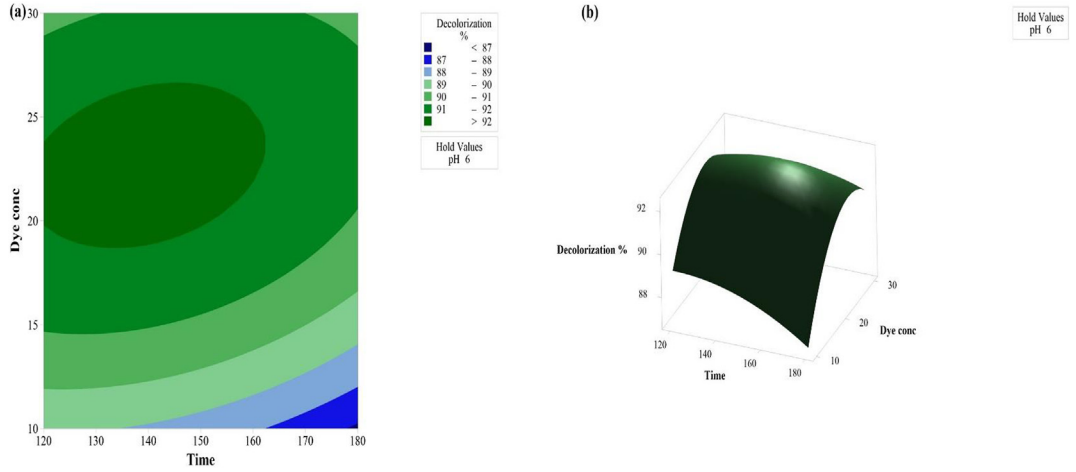

Figure 2. Contour plot and response surface plot showing interaction between time and dye concentration.

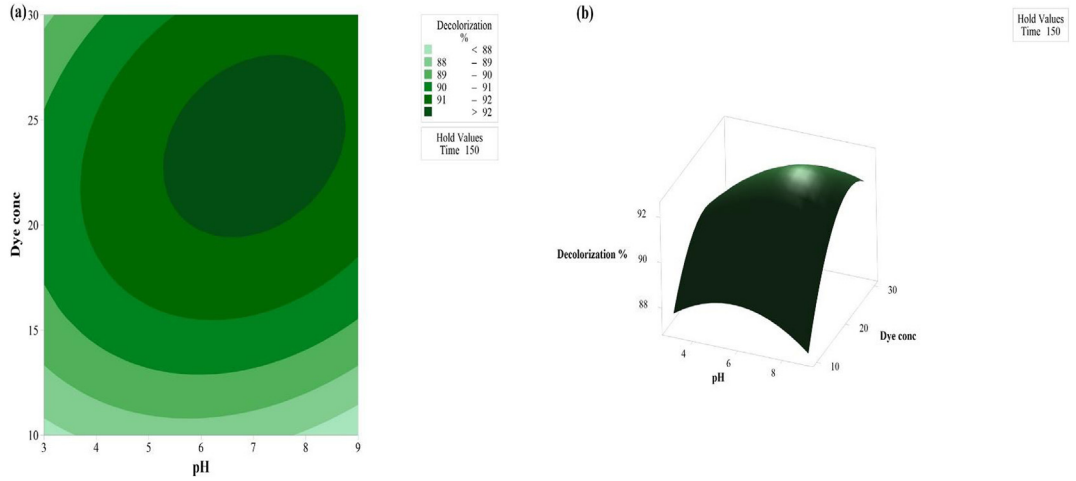

Figure 3. Contour plot and response surface plot showing interaction between pH and dye concentration.

decolorization through biosorption due to the attraction of charged dyes onto the surface of the adsorbent. An increase in the concentration of H^+ ions (acidic) attracts anionic dyes while an increase in the concentration of OH^- ions (basic) attracts cationic dyes towards the biomass surface due to electrostatic force of attraction (Ashraf et al., 2006). A decrease in the decolorization efficiency was found when there was an increase in the time from 120 to 152 min. The response surface plot showed a clear peak and the corresponding contour plot showed a diagonally elongated uniform design implying that the interaction between the pH and time was significant on dye decolorization.

Figure 2 (a and b) shows the graphical representation indicating the combined effects of dye concentration and time on dye decolorization while the pH was set at its zero levels (pH = 6). From the contour plot Figure 2 (a and b), it was clear that the decolorization efficiency (Y) increases with an increase in the dye concentration from 19 to 25% and reaches the maximum value and then decreases. The possible reason for the decrease in the decolorization efficiency could be due to the saturation of biomass. Saturation of biomass indicates that there were no free binding sites available for adsorption of dye (Smaranda et al., 2009). Maximum decolorization was attained within 162 min after which a decrease in decolorization could be found. The response surface plot showed a clear peak and the corresponding contour plot showed a diagonally elongated design denoting that there was a mutual interaction between the dye concentration and time and was significant.

Figure 3 (a and b) showed the interaction effects of dye concentration and pH while the time was set at its zero levels (Time = 150 min). A mutual increase in the dye concentration and pH could exert an augmented efficiency in the decolorization of dye (Y). However, the decolorization efficiency decreases over a prolonged increase in both factors. This could be due to the saturation of the available binding sites on the biomass surface. The optimum dye concentration was found to be between 19 to 25%, further increase causes a decrease in adsorption efficiency. On the other hand, an increase in the pH also played a vital role in the decolorization process. Accumulation of OH^- due to an increase in the pH 5.5 to 8.8 (acidic to basic) could be responsible influencing the binding of cationic dyes onto the surface of biomass (Ashraf et al., 2006), hence a considerable increase in decolorization could be obtained. The response surface plot implied a dome shape and the corresponding contour plot indicated a dark green colored diagonally elongated design implying that the interaction between the dye concentration and pH was significant on dye decolorization (Y). The optimized values of the parameters could be found within these regions.

The dye adsorption capacity is mainly influenced by the surface morphology of the algae and the functional groups present on its surface and reactive sites present on dye molecules (Crist et al., 1981; Sharma et al., 2018). The algal biomass was characterized using Fourier transform infrared spectrometry before and after adsorption of dye (Figure 4). There were many significant differences observed after the dye adsorption. Typically, the intensity of N–H and O–H bands at 3311.78 cm^{-1}

were decreased to 3282.84 cm^{-1} denoting an influence of hydroxyl functional group and hydrogen bond that were involved in the adsorption (Catherine et al., 2018; Du et al., 2014; Mohamed et al., 2019). The peak at 1635.64 cm^{-1} ascribed to C=C functional group was decreased to 1633.71 denoting the participation of π-π interactions in the dye uptake (Dai et al., 2018). Typical CH_3 and CH_2 bands at 1454.33 and 1425.40 cm^{-1} disappeared after dye adsorption onto biomass. Bands at 1249.87 cm^{-1} and 1149.57 responsible for aromatic ether and C–O was disappeared after dye uptake. The interaction between the adsorbent and adsorbate occurs due to three mechanisms namely electrostatic, hydrogen bond, and hydrophilic-hydrophobic interactions. The electrostatic force of attraction is a non-bonded interaction between two opposite charges of adsorbent and dye molecules. Hydrophilic and hydrophobic interactions occur due to the presence of non-polar aromatic groups between the dye and CH_3 group on the adsorbent surface (Giles et al., 1960; Vo and Lee, 2017).

In summary, hydrogen bonds and π-π interactions were involved the dye adsorption onto *Gracilaria edulis* however, more studies are required to analyze the physicochemical properties of dyes (e.g., molecule size, n-octanol, and n-hexane-water partition coefficient) and the specific mechanism involved in their adsorption (Xiao and Pignatello, 2015).

HR-SEM-EDX was used to study the morphological changes of biomasses before and after the adsorption process. The analysis was performed under several magnifications viz., 3,000X, 10,000X, and 30,000X. HR-SEM revealed that the surface of biomass before adsorption was found to be porous, vacant, and unoccupied (Figure 5 (a)). Whereas the biomass after adsorption showed the binding of dye on their surface

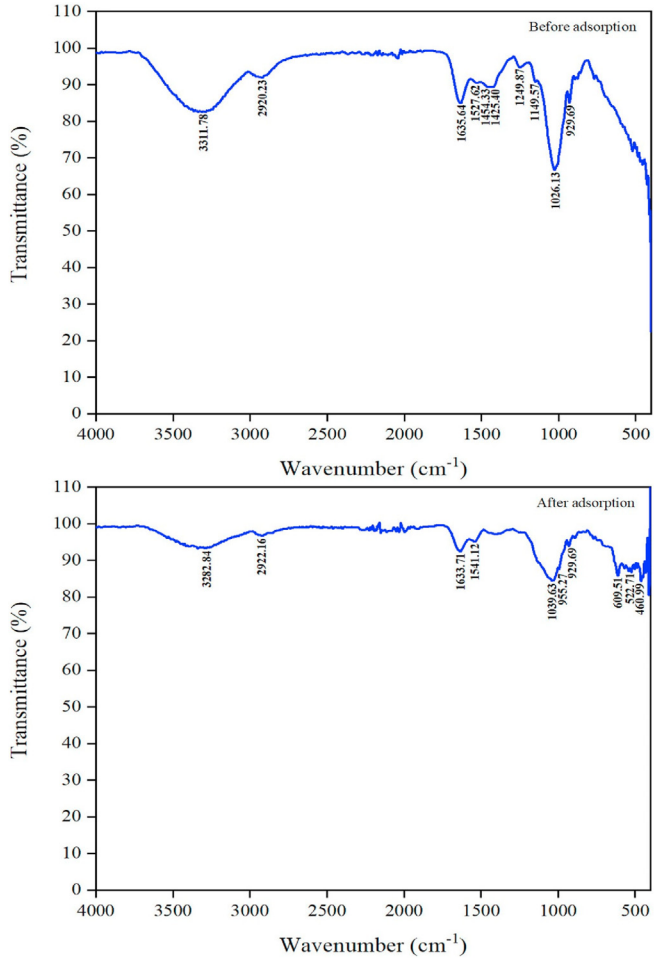

Figure 4. Fourier transform infrared spectroscopy of *Gracilaria edulis* before and after dye adsorption.

(Figure 5 (b)). Adsorption of dye on the surface of biomass is very clear from Figure 5 (b) at 3,000X magnification. This could be possible due to the electrostatic attraction between the functional groups on the biomass and charge on the dye (Ashraf et al., 2006; Namasivayam et al., 2001). EDX was employed in the study to characterize the materials accumulated on the surface of biomass. Since there is a rapid increase in the industrialization, accumulation of pollutants and heavy metals have been found everywhere. These are a potential threat to humans and the environment as they possess toxic, mutagenic, and teratogenic properties (Roeva, 1996; Scimeca et al., 2017). EDX (Figure 6) showed the presence of various elements including carbon (43.22%), oxygen (16.47%), sodium (18.54%), silicon (1.05%), sulphur (2.92%), chlorine (15.91%), potassium (0.66%), calcium (0.54%), and iron (0.68%). Thus, HR-SEM-EDX confirmed the adsorption of dye onto *Gracilaria edulis* biomass.

XRD peaks reported that biosorbent exhibited both crystalline and amorphous nature (Figure 7). The crystallinity of biomass was evident due to the presence of sharp peaks (Londoño-Restrepo et al., 2019). Table 9 denotes the mineral composition of biomass. Average crystallite size calculated using the Debye-Scherrer equation was found to be 104.19 nm. Vimala and Vedhi reported similar peaks for XRD analysis of *Gracilaria corticata* (Vimala and Vedhi, 2019) which is closely related to *Gracilaria edulis* used in the current study.

BET surface area analysis revealed the total surface area of 0.271 m^2g^{-1}, total pore volume 0.01320 cm^3g^{-1}, and mean pore diameter of 283.69 nm biomass before and 0.132 m^2g^{-1}, 0.00935 cm^3g^{-1}, and 192.66 nm after adsorption respectively (Table 10). Results obtained denotes a reduction in pore surface and pore volume significantly contributed to the adsorption process. Low surface area is often a characteristic feature of biological adsorbents and has been reported (Zhang et al., 2013). Inyinbor et al., reported a total surface area of 0.0387 m^2g^{-1} and 1.8642 m^2g^{-1} for adsorption of Rhodamine B dye using agricultural wastes (Inyinbor et al., 2015). *Gracilaria edulis* has a mean pore diameter of 283.69 nm which corresponding to micropore size (>50 nm) would have been due to the pretreatment of biomass (Hwang et al., 2018; Kumar et al., 2019). Adsorbents with such macropore sizes are rarely reported. BET isotherm and BJH pore size distribution were plotted which elucidated the adsorption and desorption properties of biomass with an increase in pressure (Figure 8). With an increase in the pressure, adsorption of inert gas onto biomass increased significantly.

3.5. Response optimization

Response optimization for the current model was performed with the target set as 99%. The optimized predicted response (decolorization percentage) was found to be 92.55% at time 131.51 min; pH 7.48; dye concentration 23.13%. The predicted optimized response was verified by performing in the wet lab experimentally. The maximum response (decolorization percentage) was found to be 92.65% (average of two trials) which was comparatively higher than the predicted response and thus proves the validity of the model.

3.6. Desorption studies

Desorption study was performed for the reusability or regeneration of the biomass in future thereby preventing the exploitation of resources since every resource has some economic importance. Natural adsorbents desorb the adsorbed dye by altering the pH of the aqueous dye solution. Desorption was done according to Mahmood (2014) with 30% (v/v) initial dye concentration under room temperature 30 ± 2 °C; 10 g/L biomass concentration; time 180 min using batch adsorption method. The pH of the solution was varied from 2 to 14 using 0.1 N HCl and 0.1 M NaOH. After the equilibrium time, the dye was filtered and biomass was dried in hot air oven (Remi RDHO-50 hot air oven) at 60 °C for 12 h and used for the study. The experiment was conducted by shaking the dye adsorbed biomass with 10 mL of distilled water (pH 7.0) in an orbital

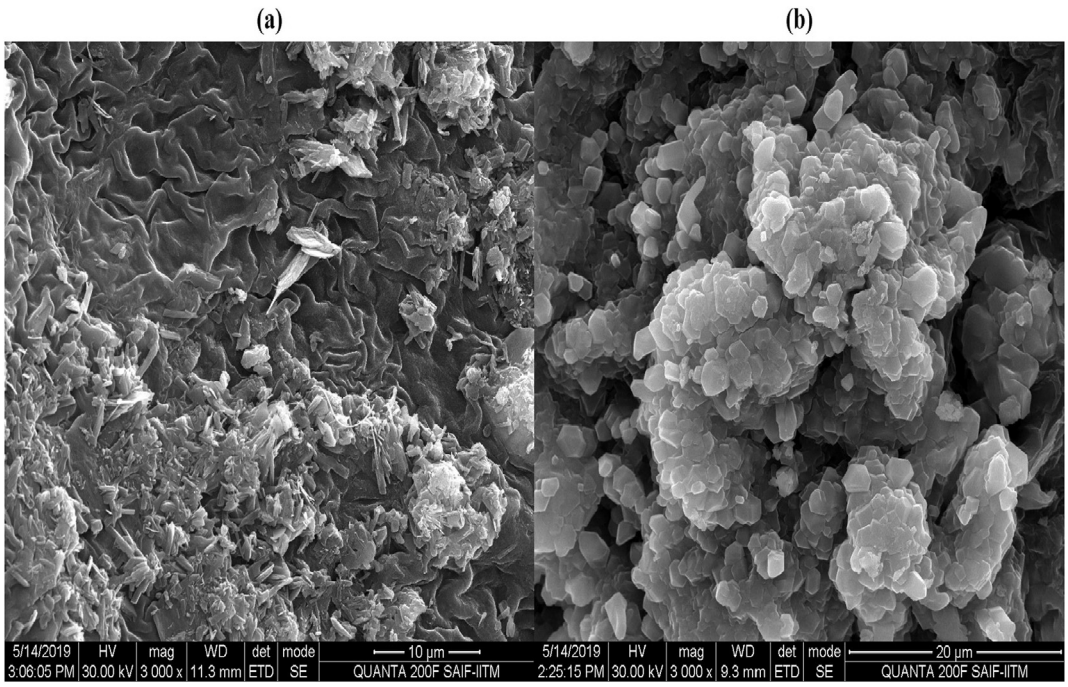

Figure 5. HR-SEM images of *Gracilaria edulis* (a) before and (b) after adsorption under 3,000X magnification.

shaker at 150 rpm for 5 min. Thirteen trials were performed similarly to determine the effect of pH on desorption. Adsorption and desorption efficiencies were analyzed spectrophotometrically at 578.8 nm Figure 9 shows the desorption of dye from adsorbed biomass at different pH and desorption efficiency was calculated using the equation (Eq. (6)).

$$\textit{Desorption (\%)} = \textit{(Desorption absorbance} - \textit{Adsorption absorbance)} * 100 \quad (6)$$

Desorption of dye was found to be highest at pH 2 with 23% possibly due to the influence of H^+ ions at acidic pH competing with dye molecules for the negatively charged binding sites on the adsorbent causing repulsion of dyes from adsorbent (Mahmood, 2014). The lowest desorption was attained at pH 14 with 13.4% efficiency. This could be due to the influence of OH^- attracting the dye towards the adsorbent due to the electrostatic force of attraction (Mahmood, 2014).

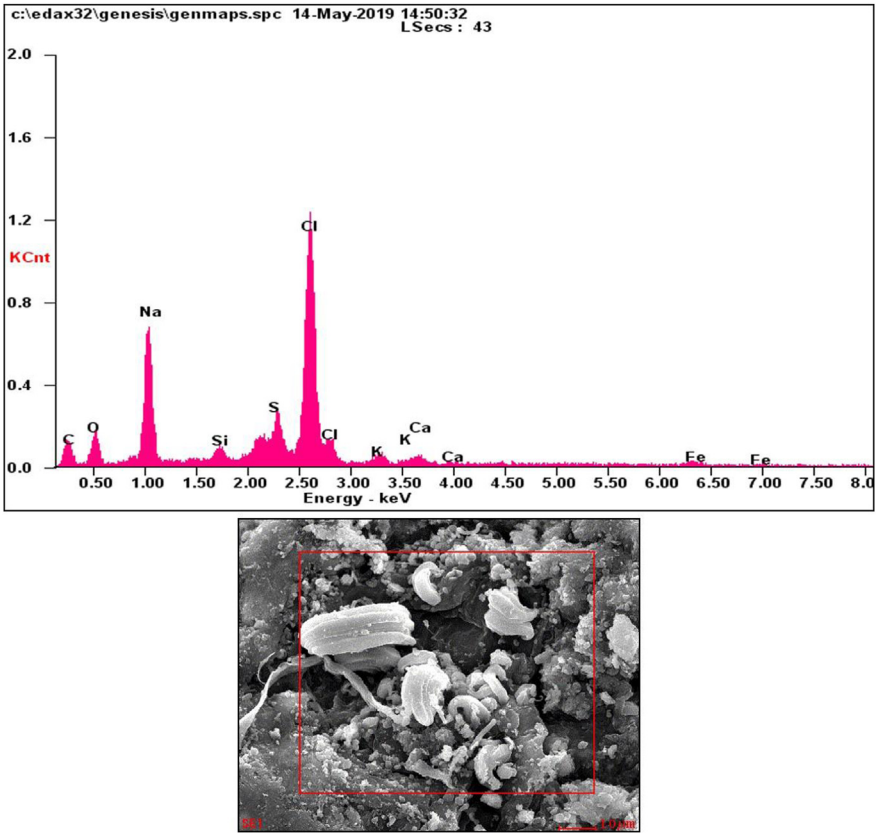

Figure 6. Energy dispersive X-ray analysis showing various elements on dye adsorbed *Gracilaria edulis*.

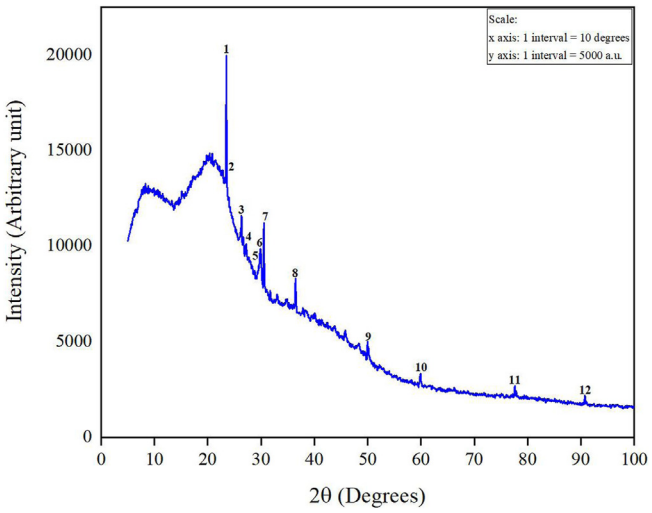

Figure 7. XRD result of *Gracilaria edulis.*

3.7. Discussion

This section discusses the findings of the previously reported similar studies that use various adsorbents for the adsorption of textile dyes. The findings of the present work is compared with every previously reported study to project the efficiency of present study. There has been a handful of studies that tested the adsorption of live industrial effluent samples containing a profusion of dyes, heavy metals, salts, acids, and other contaminants expelled from industries. The majority of the studies previously done illuminate the insights of adsorption of synthetic dyes with known concentrations, the problem lies in the removal of wastewater whose concentrations are not known such as described in the present study. The marine red macroalgae *Gracilaria edulis* was found to be a very potent biosorbent for the decolorization of textile dye effluent. Several factors like pH, temperature, biomass concentration, dye concentration, time, and static-agitation were found to influence the biosorption of dyes.

Biosorption of Crystal Violet (cationic dye) using marine red algae *Gracilaria edulis* was studied by Jegan et al. (2016). Factors such as particle size, biosorbent dosage, pH, dye concentration, and contact time, and their effects were studied by them (Jegan et al., 2016). Their maximum biosorption (decolorization) was found to be 181.0 mg/g at an optimum particle size of 1.88 mm; biosorbent dosage of 5 g/L; pH 8; dye concentration of 100 mg/L and contact time of 360 min. The current study reported 92.65% efficiency with just 1 g/L of biomass concentration. The influence of basic pH was a predominant influential factor for the adsorption of cationic onto algae. Biosorption of Basic Violet 14 onto *Gracilaria edulis* was evaluated by Devi and Murugappan. Factors like pH, biosorbent dosage, temperature, agitation speed, time, and particle size were evaluated in their study. The adsorption of dye was very rapid and has attained equilibrium at temperature 40 °C and at time 90 min. Maximum biosorption was 1250 mg/g at pH 10 was attained (Devi and Murugappan, 2016). A Pseudo-second-order model could explain their adsorption process. Devi et al. evaluated the adsorption of Reactive Blue 19 onto *Gracilaria edulis.* Parameters like pH, dye concentration, time, adsorbent concentration, agitation, biosorbent size, and temperature were optimized by them. Maximum biosorption was found to be 82.2 mg/g at pH (1.5), temperature (30 °C), time (300 min), biosorbent size (<75 mm), adsorbent concentration (1 g/L), and agitation speed (150 rpm) (Devi et al., 2015). The present study proved maximum decolorization efficiency of 92.65% could be attained which is comparable with the decolorization efficiency attained by Devi and Murugappan (2016). Sharifi and Shoja (2018) performed the biosorption of Methylene Blue onto magnesium oxide nanoparticles coated spruce sawdust using Box-Behnken design of response surface methodology reported maximum decolorization of 94% efficiency dye removal at pH 11, dye concentration of 100 mg/L, and adsorbent dosage of 3.51 g/L was attained which is comparable with the current study of 92.65% decolorization efficiency. Igwegbe et al. (2019) performed the adsorption of aqueous Methylene Blue onto Ho-$CaWO_4$ nanoparticles using CCD and artificial neural network optimization techniques. They reported a maximum of 71.17% (103.09 mg/g) decolorization efficiency was attained after at pH 2.03, time 15.16 min, adsorbent dosage 1.91 g/L, and dye concentration of 100.65 mg/L. The present study reported an efficiency higher than them.

Demirbas et al. (2008) studied the kinetic studies on adsorption of basic dye Astrazon Yellow 7GL onto the surface of apricot stone pretreated with sulphuric acid. Various operational parameters such as dye concentration, pH, sorbent dosage, time, and temperature were optimized in their study. Of the five parameters, three parameters namely

Table 9. Mineral composition of *Gracilaria edulis* using XRD.

Peak number	d (Å)	2 theta	Mineral	Crystallite size (nm)
1	3.7877	23.4677	Marialite	127.5127
2	3.7675	23.5960	Gratonite	176.7378
3	3.3803	26.3450	Ganomalite	48.3454
4	3.3377	26.6870	Olsacherite	77.2982
5	3.0238	29.5170	Denispvite	163.4509
6	2.9891	29.8670	Clinoholmquistite	20.1999
7	2.9277	30.5080	IMA 2009-010	160.0084
8	2.4626	36.4550	Palladobismutharsenide	164.0361
9	1.8236	49.9710	Nasonite	128.5861
10	1.5452	59.8020	Glagolevite	34.4340
11	1.2290	77.6210	Osmium	71.1537
12	1.0823	90.7480	Nowackiite	78.6010
				Average size = 104.19 nm

Table 10. Surface Characteristics of *Gracilaria edulis* using BET and BJH analysis.

Sample	Total surface area (BET) (m^2g^{-1})	Molar volume of gas (cm^3 (STP) g^{-1})	Total pore volume (cm^3g^{-1})	Mean pore diameter (nm)
Before adsorption	0.271	0.0631	0.01320	283.69
After adsorption	0.132	0.0303	0.00935	192.66

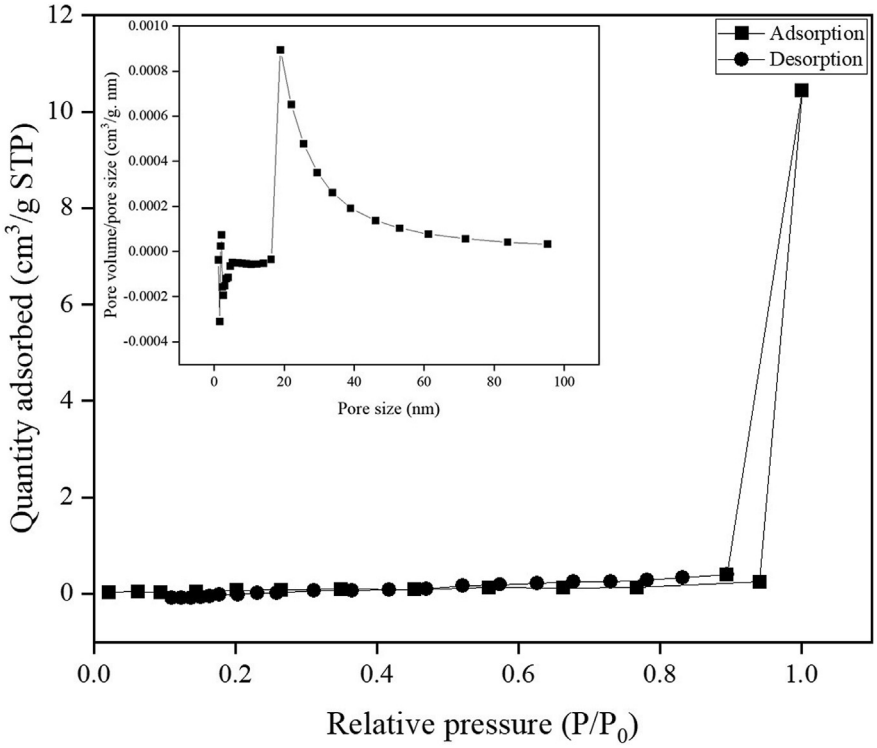

Figure 8. BET adsorption-desorption isotherm of inert N_2 onto *Gracilaria edulis* and BJH pore size distribution.

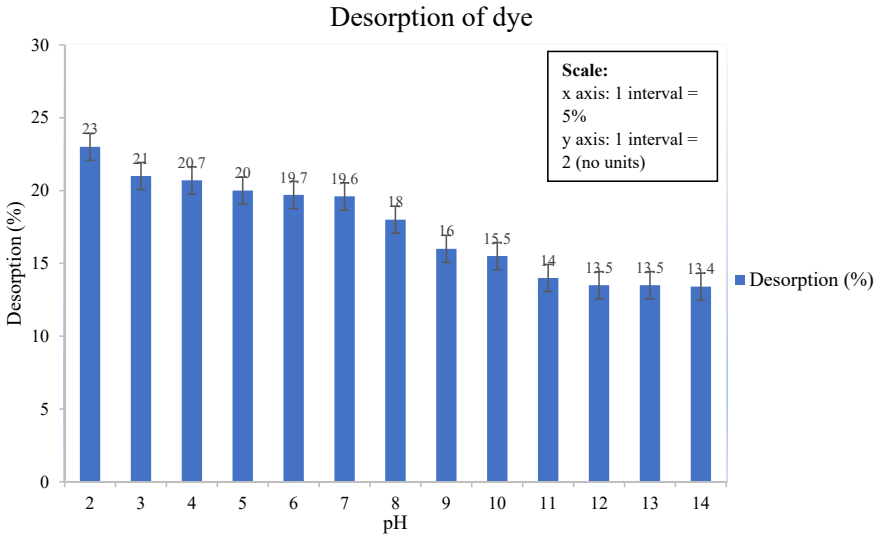

Figure 9. Desorption studies of dye adsorbed *Gracilaria edulis*.

pH, biosorbent dosage, and temperature were found to influence the adsorption process. Maximum adsorption was attained at pH 10, sorbent dosage 6 g/L, and time 35 min respectively. The data were fitted onto Langmuir and Freundlich isotherms in their study. The maximum adsorption efficiency was found to be 221.23 mg/g at 50 °C. Values of entropy and enthalpy were found to be 31.93 J/mol K and 49.87 kJ/mol indicated that the model was spontaneous and endothermic. Rozada et al. (2003) studied the adsorption of dyes onto activated carbon produced from pyrolysis of sewage sludge and chemical activation methods. Their experiment was performed using liquid-phase adsorption tests onto activated carbon. Colored aqueous dye solutions such as Methylene Blue and Safranin were used in their study. Their experiment was performed using batch and fixed-batch methods (Rozada et al., 2003). They reported that adsorption of Methylene Blue occurred faster than safranin in binary solutions nevertheless the time needed for acquiring equilibrium, fixed bed parameters, and adsorptive capacity varied for the two compounds. Sharma and Das (2012) studied the adsorption efficiency of graphene oxide nanosheets. Methyl Green, a cationic dye was used in this study and is reported to be one of the most toxic dye. Adsorption of Methyl Green onto graphene oxide nanosheet was mainly due to the presence of functional groups such as epoxy, carboxyl, and hydroxyl functional groups imparting negatively charged functional groups onto its surface. Adsorption kinetics, biomass concentration, pH (4–9), and temperature (25 °C) and their effects were studied. The adsorption mechanism and interactions were studied using various kinetic models Boyd model, Intraparticle diffusion, pseudo-first-order model, pseudo-second-order

model. The results were reported that maximum adsorption was attained at 60 min using a pseudo-second-order kinetic model. Their data were well fitted onto the Langmuir isotherm model. Enthalpy, entropy and Gibbs free energy of the experiment were also evaluated and proved that the reaction was spontaneous. Their experiment was confirmed using diffuse reflectance infrared Fourier transform spectroscopy. Oyekanmi et al. (2019) reported maximum decolorization efficiency of 89.82% and 69.96% COD reduction through adsorption of Rhodamine B dye onto acid pre-treated banana peels using CCD of RSM. Maximum decolorization and COD reduction was attained at pH 2, adsorbent dosage of 0.2 g/L and contact time of 60 min and is comparable with the efficiency of the present study with 92.65%. The experiment was best explained by Langmuir adsorption isotherm model.

Sadaf and Bhatti performed the adsorption of Indosol Yellow BG from aqueous solution onto agricultural biomass, peanut husk. The Box-Behnken design was used for their study. They reported a maximum of 58.01 mg of dye adsorbed onto 1 g of acetic acid-treated biomass at an initial concentration of 200 mg/L at pH 2, and biomass dosage of 0.17 g. They also recovered 44.5% dye from the adsorbed biomass using 1 M NaOH which is nearly double the efficiency of desorption compared to the present study (Sadaf and Bhatti, 2015). Postai and Rodrigues (2018) studied the adsorption of cationic Methylene Blue and Rhodamine B onto low-cost treated and untreated fruit waste *Eugenia umbelliflora* in a batch system. The adsorbent was characterized by them for the point of zero charge, the presence of functional groups using FTIR, and thermogravimetric properties. The adsorption process was studied using the Sips equation which best suited the model. Maximum adsorption for the untreated *Eugenia umbelliflora* was found to be 157.2 mg/g for Methylene Blue and 161.1 mg/g for Rhodamine B. Maximum adsorption efficiency for the treated *Eugenia umbelliflora* was found to be 111.6 mg/g for Methylene Blue and 106.4 mg/g for Rhodamine B. The adsorption of cationic dyes onto adsorbent followed pseudo-first-order kinetics and is comparable with the current finding with maximum decolorization of 92.65%. Their experimental model was found to be spontaneous and exothermic. The process parameters were optimized using 3-level Box-Behnken design, and the initial dye concentration was found to be the best influential factor for adsorption. The results were promising and *Eugenia umbelliflora* could be used as potential adsorbent for the large-scale dye removal process. Mahmood (2014) reported that a maximum of 13.4% was obtained at pH 12.6 for desorption of Direct Yellow 28 dye. The results of desorption reported by Mahmood (2014) is comparable with the current finding of 23% desorption efficiency. Jain et al. (2010) reported the desorption of Naphthol Yellow S from adsorbent using various concentrations of sodium hydroxide. Dilute concentrations of sodium hydroxide through a fixed bed along the adsorbent column had a significant impact on regeneration. Berez et al. (2014) reported that a maximum of 46 and 68% of Feron Blue 291 dye adsorbed onto bentonite could be desorbed using kinetic studies which is much higher than the current finding reported in this work with 23% desorption efficiency.

Thus, this section concludes by comparing the results and efficiency of the present with the previously reported different types of adsorbent materials and dyes. From the discussion, the outcomes of the present study are very efficient when compared with the adsorption potential of synthetic dyes onto several types of biomasses and further studies are to be carried out to develop small-scale commercialization.

4. Conclusion

The motive of the current study was to evaluate the influence of various factors (environmental parameters) on the decolorization of textile dye effluent through a cost-effective biosorption technique. Marine red macroalgae *Gracilaria edulis* was preferred as the biosorbent. Physical and chemical pretreatment of biomass was done to enhance the efficiency of decolorization by increasing the pore surface area and pore volume facilitating adsorption. Plackett-Burman design was used in this study to find out the important significant factors influencing the biosorption of dye effluent onto biomass. Out of six factors, three factors namely time, pH, and dye concentrations were found to exert a significant effect on the process. The three factors were further optimized using Box-Behnken of Response Surface Methodology to get the optimized values of each factor for maximum decolorization. The maximum decolorization using RSM-BB design was attained at time 130.9 min, pH 7.0, and dye concentration 16.56% respectively. The predicted (92.56%) and the experimental (92.65%) values were found to be in a good agreement under the optimized conditions. The experiment was confirmed using FTIR, HR-SEM-EDX, and BET techniques. The desorption of adsorbed dye promotes the reusability of biomass in the future. Maximum desorption of 23% from the adsorbed biomass was obtained at pH 2. Thus, by using the statistical optimization designs, we can able to save time, cost, effort, and labor spent on the conventional method of dye decolorization. In the future, *Gracilaria edulis* can be immobilized using calcium chloride and sodium alginate to promote reusability. A batch reactor can be designed to enhance the process from lab-scale to pilot-scale.

Declarations

Author contribution statement

Venkataraghavan R: Conceived and designed the experiments; Analyzed and interpreted the data; Wrote the paper.

Thiruchelvi R: Conceived and designed the experiments; Contributed reagents, materials, analysis tools or data.

Sharmila D:Performed the experiments.

Funding statement

This research did not receive any specific grant from funding agencies in the public, commercial, or not-for-profit sectors.

Competing interest statement

The authors declare no conflict of interest.

Additional information

No additional information is available for this paper.

Acknowledgements

The authors sincerely thank Vels, Institute of Science, Technology and Advanced Studies and Dr. M. Ganesan, Senior Scientist, CSIR-CSMCRI for their sincere support towards the successful completion of the research work. The authors sincerely thank the reviewers for suggesting valuable comments towards the improvement of our article to attain publishable status. The authors also thank Sophisticated instruments facility, Vellore institute of technology, Government of India and Sophisticated analytical instruments facility, Indian Institute of Technology, Madras and Department of Science and Technology and Central Instrumentation Facility, Vels Institute of Science, Technology and Advanced Studies for performing characterization studies.

References

Agarry, S.E., Ogunleye, O.O., 2012. Factorial designs application to study enhanced bioremediation of soil artificially contaminated with weathered bonny light crude oil through biostimulation and bioaugmentation strategy. J. Environ. Protect. 3, 748–759.

Aleboyeh, A., Daneshvar, N., Kasiri, M.B., 2008. Optimization of CI Acid Red 14 azo dye removal by electrocoagulation batch process with response surface methodology. Chem. Eng. Process 47, 827–832.

Amara, A.A., Salem, S.R., 2010. Logical and experimental design for phenol degradation using immobilized Acinetobacter sp. Culture. IIUM Eng. J. 11, 89–104.

Ashraf, S.S., Rauf, M.A., Alhadrami, S., 2006. Degradation of Methyl Red using Fenton's reagent and the effect of various salts. Dyes Pigments 69, 74–78.
Bai, R.S., Abraham, T.E., 2003. Studies on chromium (VI) adsorption–desorption using immobilized fungal biomass. Bioresour. Technol. 87, 17–26.
Batzias, F.A., Sidiras, D.K., 2004. Dye adsorption by calcium chloride treated beech sawdust in batch and fixed-bed systems. J. Hazard Mater. 114, 167–174.
Berez, A., Ayari, F., Abidi, N., Trabelsi-Ayadi, M., Schäfer, G., 2014. Adsorption-desorption processes of azo dye on natural bentonite: batch experiments and modelling. Clay Miner. 49, 747–763.
Brião, G.V., Jahn, S.L., Foletto, E.L., Dotto, G.L., 2018. Highly efficient and reusable mesoporous zeolite synthetized from a biopolymer for cationic dyes adsorption. Colloid Surf A Physicochem. Eng. Asp. 556, 43–50.
Catherine, H.N., Ou, M.H., Manu, B., Shih, Y.H., 2018. Adsorption mechanism of emerging and conventional phenolic compounds on graphene oxide nanoflakes in water. Sci. Total Environ. 635, 629–638.
Chaari, I., Fakhfakh, E., Medhioub, M., Jamoussi, F., 2019. Comparative study on adsorption of cationic and anionic dyes by smectite rich natural clays. J. Mol. Struct. 1179, 672–677.
Chen, Y., Huang, B., Huang, M., Cai, B., 2011. On the preparation and characterization of activated carbon from mangosteen shell. J. Taiwan Inst. Chem. Eng. 42, 837–842.
Crist, R.H., Oberholser, K., Shank, N., Nguyen, M., 1981. Nature of bonding between metallic ions and algal cell walls. Environ. Sci. Technol. 15, 1212–1217.
Cui, L., Ouyang, Y., Lou, Q., Yang, F., Chen, Y., Zhu, W., Luo, S., 2010. Removal of nutrients from wastewater with Canna indica L. under different vertical-flow constructed wetland conditions. Ecol. Eng. 36, 1083–1088.
da Cunha Oliveira, J.A., 2016. An Integrated Use of Macroalgae as Bioproducts Source and Biosorbent for Environmental Applications.
Dai, L., Zhu, W., He, L., Tan, F., Zhu, N., Zhou, Q., He, M., Hu, G., 2018. Calcium-rich biochar from crab shell: an unexpected super adsorbent for dye removal. Bioresour. Technol. 267, 510–516.
Dasgupta, J., Sikder, J., Chakraborty, S., Curcio, S., Drioli, E., 2015. Remediation of textile effluents by membrane based treatment techniques: a state of the art review. J. Environ. manage. 147, 55–72.
Demirbas, E., Kobya, M., Sulak, M.T., 2008. Adsorption kinetics of a basic dye from aqueous solutions onto apricot stone activated carbon. Bioresour. Technol. 99, 5368–5373.
Devi, S., Murugappan, A., 2016. Adsorption of basic magenta using fresh water algae and brown marine seaweed: characterization studies and error analysis. J. Eng. Sci. Technol. 11, 1421–1436.
Devi, S., Murugappan, A., Rajesh Kannan, R., 2015. Sorption of Reactive blue 19 onto freshwater algae and seaweed. Desalin. Water Treat. 54, 2611–2624.
Dhiman, P., Naushad, M., Batoo, K.M., Kumar, A., Sharma, G., Ghfar, A.A., Kumar, G., Singh, M., 2017. Nano FexZn1− xO as a tuneable and efficient photocatalyst for solar powered degradation of bisphenol A from aqueous environment. J. Clean. Prod. 165, 1542–1556.
Dong, C.H., Xie, X.Q., Wang, X.L., Zhan, Y., Yao, Y.J., 2009. Application of Box-Behnken design in optimisation for polysaccharides extraction from cultured mycelium of Cordyceps sinensis. Food Bioprod. Process. 87, 139–144.
Du, Q., Sun, J., Li, Y., Yang, X., Wang, X., Wang, Z., Xia, L., 2014. Highly enhanced adsorption of Congo red onto graphene oxide/chitosan fibers by wet-chemical etching off silica nanoparticles. Chem. Eng. J. 245, 99–106.
Dubey, A., Shiwani, S., 2012. Adsorption of lead using a new green material obtained from Portulaca plant. Int. J. Environ. Sci. Technol. 9, 15–20.
El-Naggar, N.E., Hamouda, R.A., Mousa, I.E., Abdel-Hamid, M.S., Rabei, N.H., 2018. Biosorption optimization,characterization, immobilization and application of Gelidium amansii biomass for complete Pb 2+ removal from aqueous solutions. Sci. Rep. 8, 13456.
Georgin, J., Drumm, F.C., Grassi, P., Franco, D., Allasia, D., Dotto, G.L., 2018. Potential of Araucaria angustifolia bark as adsorbent to remove Gentian Violet dye from aqueous effluents. Water Sci. Technol. 78, 1693–1703.
Giles, C.H., MacEwan, T.H., Nakhwa, S.N., Smith, D., 1960. Studies in adsorption. Part XI. A system of classification of solution adsorption isotherms, and its use in diagnosis of adsorption mechanisms and in measurement of specific surface areas of solids. J. Chem. Soc. 786, 3973–3993.
Giusto, L.A., Pissetti, F.L., Castro, T.S., Magalhães, F., 2017. Preparation of activated carbon from sugarcane bagasse soot and methylene blue adsorption. Water Air Soil Pollut. 228, 249.
Ghaly, A.E., Ananthashankar, R., Alhattab, M.V., Ramakrishnan, V.V., 2014. Production, characterization and treatment of textile effluents: a critical review. J. Chem. Eng. Process Technol. 5, 1–9.
Gupta, V.K., Nayak, A., 2012. Cadmium removal and recovery from aqueous solutions by novel adsorbents prepared from orange peel and Fe2O3 nanoparticles. Chem. Eng. J. 180, 81–90.
Hammud, H.H., Shmait, A., Hourani, N., 2015. Removal of malachite green from water using hydrothermally carbonized pine needles. RSC Adv. 5, 7909–7920.
Hanbali, M., Holail, H., Hammud, H., 2014. Remediation of lead by pretreated red algae: adsorption isotherm, kinetic, column modeling and simulation studies. Green Chem. Lett. Rev. 7, 342–358.
Haroon, M., Wang, L., Yu, H., Ullah, R.S., Khan, R.U., Chen, Q., Liu, J., 2018. Synthesis of carboxymethyl starch-g-polyvinylpyrolidones and their properties for the adsorption of Rhodamine 6G and ammonia. Carbohydr. Polym. 186, 150–158.
Harrelkas, F., Azizi, A., Yaacoubi, A., Benhammou, A., Pons, M.N., 2009. Treatment of textile dye effluents using coagulation–flocculation coupled with membrane processes or adsorption on powdered activated carbon. Desalination 235, 330–339.
Holzwarth, U., Gibson, N., 2011. The Scherrer equation versus the 'Debye-Scherrer equation. Nat. Nanotechnol. 6, 534.
Hu, X.S., Liang, R., Sun, G., 2018. Super-adsorbent hydrogel for removal of methylene blue dye from aqueous solution. J. Mater. Chem. A. 6, 17612–17624.
Hwang, K., Kwon, G.J., Yang, J., Kim, M., Hwang, W., Youe, W., Kim, D.Y., 2018. Chlamydomonas angulosa (Green Alga) and Nostoc commune (Blue-Green Alga) microalgae-cellulose composite aerogel beads: manufacture, physicochemical characterization, and Cd (II) adsorption. Materials 11, 562.
Iftekhar, S., Srivastava, V., Hammouda, S.B., Sillanpää, M., 2018. Fabrication of novel metal ion imprinted xanthan gum-layered double hydroxide nanocomposite for adsorption of rare earth elements. Carbohydr. Polym. 194, 274–284.
Igwegbe, C.A., Mohmmadi, L., Ahmadi, S., Rahdar, A., Khadkhodaiy, D., Dehghani, R., Rahdar, S., 2019. Modeling of adsorption of methylene blue dye on Ho-CaWO4 nanoparticles using response surface methodology (RSM) and artificial neural network (ANN) techniques. MethodsX 6, 1779–1797.
Inyinbor, A.A., Adekola, F.A., Olatunji, G.A., 2015. Adsorption of rhodamine B dye from aqueous solution on Irvingia gabonensis biomass: kinetics and thermodynamics studies. S. Afr. J. Chem. 68, 115–125.
Jabeen, H., Iqbal, S., Anwar, S., Parales, R.E., 2015. Optimization of profenofos degradation by a novel bacterial consortium PBAC using response surface methodology. Int. Biodeterior. Biodegrad. 100, 89–97.
Jain, R., Gupta, V.K., Sikarwar, S., 2010. Adsorption and desorption studies on hazardous dye Naphthol Yellow S. J. Hazard Mater. 182, 749–756.
Janus, M., Choina, J., Kusiak, E., Morawski, A.W., 2008. Study of nitrogen-modified titanium dioxide as an adsorbent for azo dyes. Adsorpt. Sci. Technol. 26, 501–513.
Jegan, J., Vijayaraghavan, J., Pushpa, T.B., Basha, S.J.S., 2016. Application of seaweeds for the removal of cationic dye from aqueous solution. Desalin. Water Treat. 57, 25812–25821.
Jo, J.H., Lee, D.S., Park, D., Choe, W.S., Park, J.M., 2008. Optimization of key process variables for enhanced hydrogen production by Enterobacter aerogenes using statistical methods. Bioresour. Technol. 99, 2061–2066.
Kabbout, Rana., Taha, S., 2014. Biodecolorization of textile dye effluent by biosorption on fungal biomass materials. Phys. Procedia. 55, 437–444.
Kang, J.X., Chen, T.W., Zhang, D.F., Guo, L., 2016. PtNiAu trimetallic nanoalloys enabled by a digestive-assisted process as highly efficient catalyst for hydrogen generation. Nano energy 23, 145–152.
Khan, T.A., Nazir, M., 2015. Enhanced adsorptive removal of a model acid dye bromothymol blue from aqueous solution using magnetic chitosan-bamboo sawdust composite: batch and column studies. Environ. Prog. Sustain. Energy 34, 1444–1454.
Kharat, D.S., 2015. Preparing agricultural residue based adsorbents for removal of dyes from effluents-a review. Braz. J. Chem. Eng. 32, 1–12.
Koocheki, A., Taherian, A.R., Razavi, S.M., Bostan, A., 2009. Response surface methodology for optimization of extraction yield, viscosity, hue and emulsion stability of mucilage extracted from Lepidium perfoliatum seeds. Food Hydrocolloids 23, 2369–2379.
Kumar, M., Goswami, L., Singh, A.K., Sikandar, M., 2019. Valorization of coal fired-fly ash for potential heavy metal removal from the single and multi-contaminated system. Heliyon 5, e02562.
Lakshmikandan, M., Sivaraman, K., Raja, S.E., Vasanthakumar, P., Rajesh, R.P., Sowparthani, K., Jebasingh, S.E., 2014. Biodegradation of acrylamide by acrylamidase from Stenotrophomonas acidaminiphila MSU12 and analysis of degradation products by MALDI-TOF and HPLC. Int. Biodeterior. Biodegrad. 94, 214–221.
Le Man, H., Behera, S.K., Park, H.S., 2010. Optimization of operational parameters for ethanol production from Korean food waste leachate. Int. J. Environ. Sci. Technol. 7, 157–164.
Leusch, A., Holan, Z.R., Volesky, B., 1995. Biosorption of heavy metals (Cd, Cu, Ni, Pb, Zn) by chemically-reinforced biomass of marine algae. J. Chem. Technol. Biotechnol. 62, 279–288.
Li, T., Shu, Z., Zhou, J., Chen, Y., Yu, D., Yuan, X., Wang, Y., 2015. Template-free synthesis of kaolin-based mesoporous silica with improved specific surface area by a novel approach. Appl. Clay Sci. 107, 182–187.
Londoño-Restrepo, S.M., Jeronimo-Cruz, R., Millán-Malo, B.M., Rivera-Muñoz, E.M., Rodriguez-García, M.E., 2019. Effect of the nano crystal size on the X-ray diffraction patterns of biogenic hydroxyapatite from human, bovine, and porcine bones. Sci. Rep. 9, 5915.
Machado, F.M., Bergmann, C.P., Fernandes, T.H., Lima, E.C., Royer, B., Calvete, T., Fagan, S.B., 2011. Adsorption of Reactive Red M-2BE dye from water solutions by multi- walled carbon nanotubes and activated carbon. J. Hazard Mater. 192, 1122–1131.
Mahmood, S., 2014. Adsorption/desorption of Direct Yellow 28 on apatitic phosphate: mechanism, kinetic and thermodynamic studies. J. Assoc. Arab Univ. Basic Appl. Sci. 16, 64–73.
Mohamed, H.S., Soliman, N.K., Abdelrheem, D.A., Ramadan, A.A., Elghandour, A.H., Ahmed, S.A., 2019. Adsorption of Cd2+ and Cr3+ ions from aqueous solutions by using residue of Padina gymnospora waste as promising low-cost adsorbent. Heliyon 5, e01287.
Moscofian, A.S., Pires, C.T., Vieira, A.P., Airoldi, C., 2012. Organofunctionalized magnesium phyllosilicates as mono-or bifunctitonal entities for industrial dyes removal. RSC Adv. 2, 3502–3511.
Namasivayam, C., Radhika, R., Suba, S., 2001. Uptake of dyes by a promising locally available agricultural solid waste: coir pith. Waste Manag. 21, 381–387.
Ngulube, T., Gumbo, J.R., Masindi, V., Maity, A., 2017. An update on synthetic dyes adsorption onto clay based minerals: a state-of-art review. J. Environ. Manag. 191, 35–57.
Oyekanmi, A.A., Ahmad, A., Hossain, K., Rafatullah, M., 2019. Adsorption of Rhodamine B dye from aqueous solution onto acid treated banana peel: response surface methodology, kinetics and isotherm studies. PloS One 14, e0216878.

Parmar, N.D., Shukla, S.R., 2018. Decolourization of dye wastewater by microbial methods-A review. Indian J. Chem. Technol. 25, 315–323.
Piai, L., Blokland, M., van der Wal, A., Langenhoff, A., 2020. Biodegradation and adsorption of micropollutants by biological activated carbon from a drinking water production plant. J. Hazard Mater. 388, 122028.
Plackett, Robin, L., Burman, J.P., 1946. The design of optimum multifactorial experiments. Biometrika 33, 305–325.
Popoola, L.T., 2019. Nano-magnetic walnut shell-rice husk for Cd (II) sorption: design and optimization using artificial intelligence and design expert. Heliyon 5, e02381.
Postai, D.L., Rodrigues, C.A., 2018. Adsorption of cationic dyes using waste from fruits of Eugenia umbelliflora Berg (Myrtaceae). Arabian J. Sci. Eng. 43, 2425–2440.
Priyadharshini, S.D., Bakthavatsalam, A.K., 2016. Optimization of phenol degradation by the microalga chlorella pyrenoidosa using plackett–burman design and response surface methodology. Bioresour. Technol. 207, 150–156.
Rai, A., Mohanty, B., Bhargava, R., 2016. Supercritical extraction of sunflower oil: a central composite design for extraction variables. Food Chem. 192, 647–659.
Ramesh, T.N., Kirana, D.V., Ashwini, A., Manasa, T.R., 2017. Calcium hydroxide as low cost adsorbent for the effective removal of indigo carmine dye in water. J. Saudi Chem. Soc. 21, 165–171.
Roeva, N.N., 1996. Special features of the behavior of heavy metals in various natural environments. J. Anal. Chem. 51, 352–364.
Romauld, S.I., Venkataraghavan, R., Yuvaraj, D., Devi, V.I., Hashika, S., 2019. Mycoremediation of Hydrocarbon and its products using Fusarium oxysporum. Res. J. Pharm. Technol. 12, 4216–4224.
Rozada, F., Calvo, L.F., Garcıa, A.I., Martın-Villacorta, J., Otero, M., 2003. Dye adsorption by sewage sludge-based activated carbons in batch and fixed-bed systems. Bioresour. Technol. 87, 221–230.
Sadaf, S., Bhatti, H.N., 2015. Response surface methodology approach for optimization of adsorption process for the removal of Indosol Yellow BG dye from aqueous solution by agricultural waste. Desalin. Water Treat. 57, 11773–11781.
Scimeca, M., Feola, M., Romano, L., Rao, C., Gasbarra, E., Bonanno, E., Brandi, M.L., Tarantino, U., 2017. Heavy metals accumulation affects bone microarchitecture in osteoporotic patients. Environ. Toxicol. 32, 1333–1342.
Sharifi, S.H., Shoja, H., 2018. Optimization of process variables by response surface methodology for methylene blue dye removal using Spruce sawdust/MgO nano-biocomposite. J. Water Environ. Nanotechnol. 3, 157–172.
Sharma, G., Dionysiou, D.D., Sharma, S., Kumar, A., Ala'a, H., Naushad, M., Stadler, F.J., 2019. Highly efficient Sr/Ce/activated carbon bimetallic nanocomposite for photoinduced degradation of rhodamine B. Catal. Today 335, 437–451.
Sharma, G., Gupta, V.K., Agarwal, S., Bhogal, S., Naushad, M., Kumar, A., Stadler, F.J., 2018a. Fabrication and characterization of trimetallic nano-photocatalyst for remediation of ampicillin antibiotic. J. Mol. Liq. 260, 342–350.
Sharma, G., Kumar, A., Devi, K., Sharma, S., Naushad, M., Ghfar, A.A., Ahamad, T., Stadler, F.J., 2018b. Guar gum-crosslinked-Soya lecithin nanohydrogel sheets as effective adsorbent for the removal of thiophanate methyl fungicide. Int. J. Biol. Macromol. 114, 295–305.
Sharma, G., Kumar, A., Naushad, M., García-Peñas, A., Ala'a, H., Ghfar, A.A., Sharma, V., Ahamad, T., Stadler, F.J., 2018c. Fabrication and characterization of Gum Arabic-cl-poly (acrylamide) nanohydrogel for effective adsorption of crystal violet dye. Carbohydr. Polym. 202, 444–453.
Sharma, G., Naushad, M., Ala'a, H., Kumar, A., Khan, M.R., Kalia, S., Bala, M., Sharma, A., 2017a. Fabrication and characterization of chitosan-crosslinked-poly (alginic acid) nanohydrogel for adsorptive removal of Cr (VI) metal ion from aqueous medium. Int. J. Biol. Macromol. 95, 484–493.
Sharma, G., Thakur, B., Naushad, M., Ala'a, H., Kumar, A., Sillanpaa, M., Mola, G.T., 2017b. Fabrication and characterization of sodium dodecyl sulphate@ ironsilicophosphate nanocomposite: ion exchange properties and selectivity for binary metal ions. Mater. Chem. Phys. 193, 129–139.
Sharma, G., Thakur, B., Naushad, M., Kumar, A., Stadler, F.J., Alfadul, S.M., Mola, G.T., 2018d. Applications of nanocomposite hydrogels for biomedical engineering and environmental protection. Environ. Chem. Lett. 16, 113–146.
Sharma, P., Das, M.R., 2012. Removal of a cationic dye from aqueous solution using graphene oxide nanosheets: investigation of adsorption parameters. J. Chem. Eng. Data 58, 151–158.
Silveira, J.E., Zazo, J.A., Pliego, G., Bidóia, E.D., Moraes, P.B., 2015. Electrochemical oxidation of landfill leachate in a flow reactor: optimization using response surface methodology. Environ. Sci. Pollut. Res. 22, 5831–5841.
Sivasubramanian, S., Namasivayam, S.K., 2015. Phenol degradation studies using microbial consortium isolated from environmental sources. J. Environ. Chem. Eng. 3, 243–252.
Smaranda, C., Bulgariu, D., Gavrilescu, M., 2009. An investigation of the sorption of Acid Orange 7 from aqueous solution onto soil. Environ. Eng. Manage. J. 8, 1391–1402.
Suhaila, Y.N., Ramanan, R.N., Rosfarizan, M., Latif, I.A., Ariff, A.B., 2013. Optimization of parameters for improvement of phenol degradation by Rhodococcus UKMP-5M using response surface methodology. Ann. Microbiol. 63, 513–521.
Sui, J., Wang, L., Zhao, W., Hao, J., 2016. Iron–naphthalenedicarboxylic acid gels and their high efficiency in removing arsenic (v). Chem. Commun. 52, 6993–6996.
Ungureanu, C.P., Favier, L., Bahrim, G., Amrane, A., 2015. Response surface optimization of experimental conditions for carbamazepine biodegradation by Streptomyces MIUG 4.89. N. Biotech. 32, 347–357.
Vakili, M., Rafatullah, M., Salamatinia, B., Abdullah, A.Z., Ibrahim, M.H., Tan, K.B., Gholami, Z., Amouzgar, P., 2014. Application of chitosan and its derivatives as adsorbents for dye removal from water and wastewater: a review. Carbohydr. Polym. 113, 115–130.
Venkataraghavan, R., Thiruchelvi, R., 2019. Screening of process parameters influencing the biosorption of textile effluents using plackett-burman design. Indian J. Environ. Protect. 39, 712–718.
Vijayaraghavan, J., Basha, S.S., Jegan, J., 2013. A review on efficacious methods to decolorize reactive azo dye. J. Urban Environ. Eng. 7, 30–47.
Vimala, A., Vedhi, C., 2019. Electrochemical sensors for heavy metals detection in Gracilaria corticata using multiwalled carbon nanotubes modified glassy carbon electrode. J. Anal. Chem. 74, 276–285.
Vo, D.T., Lee, C.K., 2017. Hydrophobically modified chitosan sponge preparation and its application for anionic dye removal. J. Environ. Chem. Eng. 5, 5688–5694.
Wang, S., Peng, Y., 2010. Natural zeolites as effective adsorbents in water and wastewater treatment. Chem. Eng. J. 156, 11–24.
Xiao, F., Pignatello, J.J., 2015. π+–π Interactions between (Hetero) aromatic Amine cations and the graphitic surfaces of pyrogenic carbonaceous materials. Environ. Sci. Technol. 49, 906–914.
Xu, P., Fu, H., Au, O.K., Tai, C.L., 2012. Lazy selection: a scribble-based tool for smart shape elements selection. ACM Trans. Graph. 31, 1–9.
Yang, Y., Yu, W., He, S., Yu, S., Chen, Y., Lu, L., Shu, Z., Cui, H., Zhang, Y., Jin, H., 2019. Rapid adsorption of cationic dye-methylene blue on the modified montmorillonite/ graphene oxide composites. Appl. Clay Sci. 168, 304–311.
Zafar, M.N., Parveen, A., Nadeem, R., 2013. A pretreated green biosorbent based on Neem leaves biomass for the removal of lead from wastewater. Desalin. Water Treat. 51, 4459–4466.
Zhang, R., Zhou, Y., Gu, X., Lu, J., 2015. Competitive adsorption of methylene blue and Cu2+ onto citric acid modified pine sawdust. Clean 43, 96–103.
Zhang, Z., O'Hara, I.M., Kent, G.A., Doherty, W.O., 2013. Comparative study on adsorption of two cationic dyes by milled sugarcane bagasse. Ind. Crop. Prod. 42, 41–49.
Zhou, J., Yu, X., Ding, C., Wang, Z., Zhou, Q., Pao, H., Cai, W., 2011. Optimization of phenol degradation by Candida tropicalis Z-04 using Plackett-Burman design and response surface methodology. J. Environ. Sci. 23, 22–30.
Zhou, X., Liu, D., Bu, H., Deng, L., Liu, H., Yuan, P., Du, P., Song, H., 2018. XRD-based quantitative analysis of clay minerals using reference intensity ratios, mineral intensity factors, Rietveld, and full pattern summation methods: a critical review. Solid Earth Sci. 3, 16–29.